

11-25-2003

# Nucleotide and Phospholipid-dependent Control of PPXD and C-domain Association for SecA ATPase

Don Oliver

Wesleyan University, [doliver@wesleyan.edu](mailto:doliver@wesleyan.edu)

Follow this and additional works at: <http://wescholar.wesleyan.edu/div3facpubs>



Part of the [Molecular Biology Commons](#)

---

## Recommended Citation

Oliver, Don, "Nucleotide and Phospholipid-dependent Control of PPXD and C-domain Association for SecA ATPase" (2003).

*Division III Faculty Publications*. Paper 92.

<http://wescholar.wesleyan.edu/div3facpubs/92>

This Article is brought to you for free and open access by the Natural Sciences and Mathematics at WesScholar. It has been accepted for inclusion in Division III Faculty Publications by an authorized administrator of WesScholar. For more information, please contact [dschnaidt@wesleyan.edu](mailto:dschnaidt@wesleyan.edu), [ljohnson@wesleyan.edu](mailto:ljohnson@wesleyan.edu).

## Nucleotide and Phospholipid-Dependent Control of PPXD and C-Domain Association for SecA ATPase<sup>†</sup>

Haiyuan Ding, Ishita Mukerji, and Donald Oliver\*

Department of Molecular Biology and Biochemistry, Wesleyan University, Middletown, Connecticut 06459, USA

Received June 26, 2003; Revised Manuscript Received August 13, 2003

**ABSTRACT:** The SecA ATPase motor is a central component of the eubacterial protein translocation machinery. It is comprised of N- and C-domain substructures, where the N-domain is comprised of two nucleotide-binding domains that flank a preprotein-binding domain (PPXD), while the C-domain binds phospholipids as well as SecB chaperone. Our recent crystal structure of *Bacillus subtilis* SecA protomer [Hunt, J. F., Weinkauff, S., Henry, L., Fak, J. J., McNicholas, P., Oliver, D. B., and Deisenhofer, J. (2002) *Science* 297, 2018–2026] along with experimental support for the correct dimer structure [Ding, H., Hunt, J. F., Mukerji, I., and Oliver, D. (2003) *Biochemistry* 42, 8729–8738] have now allowed us to study SecA structural dynamics during interaction with various translocation ligands and to relate these findings to current models of SecA-dependent protein translocation. In this paper, we utilized fluorescence resonance energy transfer methodology with genetically engineered SecA proteins containing unique pairs of tryptophan and fluorophore-labeled cysteine residues within the PPXD and C-domains of SecA to investigate the interaction of these two domains and their response to temperature, model membranes, and nucleotide. Consistent with the crystal structure of SecA, we found that the PPXD and C-domains are proximal to one another in the ground state. Increasing temperature or binding to model membranes promoted a loosening of PPXD and C-domain association, while ADP binding promoted a tighter association. A similar pattern of PPXD and C-domain association was obtained also for *Escherichia coli* SecA protein. Furthermore, a hyperactive Azi-PrfD SecA protein of *E. coli* had increased PPXD and C-domain separation, consistent with its activation in the ground state. Interestingly, PPXD and C-domain separation occurred prior to the onset of major temperature-induced conformational changes in both the PPXD and C-domains of SecA. Our results support a model in which PPXD and C-domain proximity is important for regulating the initial stages of SecA activation, and they serve also as a template for future structural studies aimed at elucidation of the chemomechanical cycle of SecA-dependent protein translocation.

In *Escherichia coli*, Sec-dependent protein transport is the major pathway responsible for the biogenesis of both secretory and many integral membrane proteins. This system consists of the cytosolic SecB chaperone, the SecA translocation ATPase, integral membrane SecYE protein, the SecA membrane receptor that appears to comprise the translocation channel, and integral membrane accessory proteins SecG and SecDF that enhance the basic translocation process (1–4). SecA is the central player of this system, which makes a number of interactions with critical components of the translocation machinery including ATP, the substrate presecretory or membrane protein, SecB, SecYE, SecG, and anionic phospholipids (5–14). Numerous studies suggest that conformational changes of SecA during interaction with its various translocation ligands promote its function.

SecA ATPase is a large multifunctional protein, whose crystal structure for the *Bacillus subtilis* enzyme has been solved recently (15). High and low affinity nucleotide-binding domains (NBF-I and NBF-II, respectively, see Figure 1) flank a preprotein-binding domain (PPXD) based on cross-linking studies and are located in the proximal two-thirds of SecA, which is collectively referred to as the N-domain (6, 7, 16, 17). The C-terminal one-third of SecA is termed the C-domain. It consists of  $\alpha$ -helical scaffold and wing domains that are important organizing centers for SecA dimer along with a C-terminal linker that contains phospholipid and SecB binding sites (18).

Since SecA interacts with numerous ligands in a concerted manner, it is important to understand the nature of interdomain communication within this complex protein. We chose to begin this task by investigating the interaction between the PPXD and C-domains of SecA and their response to various translocation ligands. The PPXD domain was originally identified as a region that specifically cross-linked to preproteins utilizing a set of overlapping fragments of SecA dimer (7). More recent analysis has defined a smaller region (residues 219–244) of *E. coli* SecA that is necessary for signal peptide binding (17). In addition, Tyr326 has been

<sup>†</sup> This work was supported by Grants GM42033 from the National Institutes of Health to D.O., and the Patrick and Catherine Weldon Donaghue Medical Research Foundation (DF#00-118) and the National Science Foundation (MCB-9507241) to I.M.

\* Corresponding author: Phone: (860) 685–3556; fax: (860) 685–2141; e-mail: doliver@wesleyan.edu.

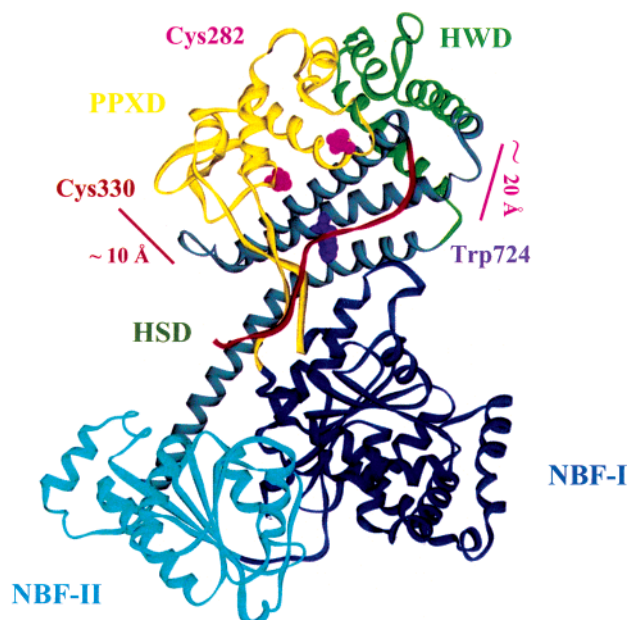


FIGURE 1: FRET pairs utilized in this study. Stereo ribbon diagrams of the *B. subtilis* SecA crystal structure are shown color-coded according to domain organization (15). The first nucleotide-binding fold (NBF-I) is shown in dark blue, the second nucleotide-binding fold (NBF-II) is in cyan, the preprotein cross-linking domain (PPXD) is in yellow, the  $\alpha$ -helical scaffold domain (HSD) is in dark green, the  $\alpha$ -helical wing domain (HWD) is in light green, and the C-terminal linker (CTL) is in red. The side-chains of the residues used for the FRET experiments are shown in space-filling representations. The lines give an approximate indication of the separation between Trp724 in HWD and the two cysteine sites (Cys282 and Cys330) in PPXD.

shown to be important for controlling preprotein interaction with *E. coli* SecA (19).

The C-domain of SecA was first defined as a translocation-dependent and membrane-protected 30-kDa protease resistant fragment (20, 21). Additional studies indicated that the C-domain is also responsible for the conformational switch between the more compact form of SecA that is favored at low temperature or upon ADP binding (i.e., the ground state) and a more extended or open conformation that is favored at high temperature or upon binding adenylyl imidodiphosphate (a nonhydrolyzable ATP analogue), preproteins, or model membranes containing anionic phospholipids (5, 13, 22, 23). This reversible change in SecA conformation that can be induced by temperature has been referred to as its endothermic transition (13).

Several lines of evidence suggest interdomain communication between the PPXD and C-domains of SecA. Initial studies of the effect of translocation ligands on the pattern of SecA protease sensitivity indicated that ADP stabilized a 95-kDa protease-resistant fragment of SecA, while preprotein or signal peptide and anionic phospholipids were destabilizing (5, 8). Later it was shown by more direct means that signal peptide binding to SecA enhanced the conformational change within the C-domain that results in its endothermic transition and enhanced proteolysis (23, 24). Recent studies have also shown that truncated SecA derivatives lacking the C-domain possess increased affinity for signal peptides as well as higher ATPase activity at NBF-I (17, 25). A site within the C-domain (around residues 783–795) termed the intramolecular regulator of ATP hydrolysis (IRA1) has been

localized that is required for these normally repressive effects of the C-domain on the other two domains of SecA (17, 26).

In this study, we have made use of fluorescence resonance energy transfer methodology to assess PPXD and C-domain association and the effects of temperature, nucleotide, and model membranes on their interaction. This approach has been widely used to examine conformational changes within proteins (for recent examples, see refs 27 and 28). Common donor–acceptor strategies for proteins include the use of an intrinsic natural fluorophore, usually Trp, and an extrinsic label, introduced through covalent attachment to a Cys residue. Our previous work employed this methodology to provide experimental evidence in favor of an antiparallel dimer structure for SecA protein (29). In the present study, this approach was utilized to examine a model in which PPXD and C-domain proximity and its modulation by temperature and translocation ligands are important for regulating SecA activation during the initial stages of protein translocation.

## EXPERIMENTAL PROCEDURES

**Chemicals.** MIANS<sup>1</sup> and tris(2-carboxyethyl)phosphine hydrochloride were purchased from Molecular Probes (Eugene, OR). DOPE and DOPG were purchased from Avanti Polar Lipids (Pelham, AL), and ADP was from Sigma (St. Louis, MO).

**Mutagenesis.** Plasmids overproducing *B. subtilis* SecA protein derivatives, pT7div-W652, pT7div-W724, pT7div-W724–C4, and pT7div-W724–C282, or an *E. coli* SecA protein derivative, pT7secA-S300C, have been described previously (29, 30). Starting with plasmid pT7div-W724–C4 lacking any Cys residues pT7div-W724–C330 was constructed by substitution mutagenesis utilizing appropriate oligonucleotide primers and a Quik-Change site-directed mutagenesis kit (Stratagene) as described by the manufacturer. Plasmid pT7 secA-Y134S–S300C was constructed similarly starting from pT7 secA-S300C.

**Purification of SecA Proteins, Preparation of LUV, and ATPase Assays.** SecA proteins were overproduced from BL21.19 containing the appropriate plasmid and purified as described previously (29). Protein purity was assessed by SDS–PAGE and Coomassie brilliant blue staining and was typically greater than 95%. Protein concentration was determined using the Bradford assay (BioRad) with bovine serum albumin as a standard. LUV composed of 30% DOPE and 70% DOPG were made by the filter extrusion method as described previously (23). SecA ATPase activities were determined by the Malachite green method (31) utilizing the modifications described previously (6). ATPase activity was calculated as previously reported (6).

**MIANS Labeling.** SecA (0.3 mg/mL) in TKE buffer (25 mM Tris-HCl, pH 7.5, 25 mM KCl, 1 mM EDTA) was incubated on ice for 0.5–1 h with 30  $\mu$ M tris(2-carboxyethyl)phosphine hydrochloride when a 4-fold molar excess of MIANS was added and the mixture was incubated on ice in the dark for an additional 3–4 h. The reaction was

<sup>1</sup> Abbreviations: DOPE, 1,2-dioleoyl-*sn*-glycerol-3-phosphoethanolamine; DOPG, 1,2-dioleoyl-*sn*-glycerol-3 [phospho-*rac*-(1-glycerol)]; FRET, fluorescence resonance energy transfer; LUV, large unilamellar vesicles; MIANS, 2-(4'-maleimidyl)anilino)naphthalene-6-sulfonic acid; PPXD, preprotein cross-linking domain.

quenched by addition of a 10-fold molar excess of  $\beta$ -mercaptoethanol. The mixture was applied to a G-25 Sephadex column PD-10 (Pharmacia) and the void volume was collected to remove any free or  $\beta$ -mercaptoethanol-reacted MIANS. The SecA labeling efficiency was calculated as follows: the MIANS concentration of the protein adduct was determined from its absorbance at 324 nm using the molar extinction coefficient of MIANS ( $\epsilon_{324\text{nm}} = 27000 \text{ M}^{-1} \text{ cm}^{-1}$ ), while the SecA concentration was determined by the Bradford assay (BioRad) with bovine serum albumin as standard. The labeling efficiency was expressed as the molar ratio of MIANS to SecA monomer  $\times 100\%$ . The labeling efficiency was typically 90–100%.

**Fluorescence Measurements.** Steady-state fluorescence spectra were recorded at 40  $\mu\text{g/mL}$  SecA protein in TKE buffer (25 mM Tris-HCl, pH 7.5, 25 mM KCl, 1 mM EDTA) on a FluoroMax-2 spectrofluorometer (Instruments S.A., Metuchen, NJ) with a Neslab programmable water bath with a remote sensor. Sample was placed in a quartz cuvette with a 1.0-cm excitation and 0.4-cm emission path length. The excitation and emission slits were set at 0.94 nm to give a 4-nm band-pass. Spectra were scanned at a rate of 1 nm/s from 320 to 450 nm using an excitation wavelength of 297 nm, or 350–550 nm when excited at 324 nm. Two or more data sets were collected for all experiments.

**Data Analysis.** All the spectra were corrected for background. The efficiency of FRET ( $E_{\text{FRET}}$ ) was calculated using the following equation (32):

$$E_{\text{FRET}} = (1 - F_{\text{DA}}/F_{\text{D}})/f_{\text{a}} \quad (1)$$

where  $F_{\text{DA}}$  and  $F_{\text{D}}$  are the Trp fluorescence of SecA in the presence and absence of MIANS labeling, respectively, and  $f_{\text{a}}$  is the fraction of labeling. The efficiency of energy transfer is related to  $R_0$ , the Förster radius, and  $R$ , the distance between donor and acceptor, by the following equation:

$$E_{\text{FRET}} = R_0^6/(R_0^6 + R^6) \quad (2)$$

$R_0$  represents the distance where the transfer is 50% efficient and is calculated (in angstroms) as follows:

$$R_0 = 0.211[n^{-4}Q_{\text{D}}\kappa^2J(\lambda)]^{1/6} \quad (3)$$

in the above equation,  $n$  is the refractive index (taken as 1.4),  $\kappa$  is the orientation factor ( $\kappa^2$  assumed to be 2/3 for randomly oriented, mobile donor, and acceptor), and  $Q_{\text{D}}$  is the quantum yield of the donor in the absence of acceptor.  $J(\lambda)$ , the overlap integral between donor emission and acceptor absorption, is calculated from the spectral data by

$$J(\lambda) = \int_0^\infty [\epsilon_{\text{A}}(\lambda)\lambda^4]f_{\text{D}}(\lambda) d\lambda \quad (4)$$

where  $\epsilon_{\text{A}}(\lambda)$  is the extinction coefficient for acceptor ( $\text{M}^{-1} \text{ cm}^{-1}$ ) and  $f_{\text{D}}$  is the fluorescence intensity of the donor at wavelength  $\lambda$  (nm).

## RESULTS

**Experimental Design and Protein Production and Labeling.** The structure of the *B. subtilis* SecA protomer (Div) has been solved recently along with obtaining direct experimental support for the antiparallel orientation of the dimer

(15, 29). To study PPXD and C-domain interaction by FRET, we utilized Div proteins that contain only one (Trp724) of two naturally occurring Trp residues within the C-domain and where the four naturally occurring Cys residues (Cys825, Cys827, Cys836, and Cys837) within the C-terminal linker domain were changed to Ser or His and a unique Cys residue (Cys282 or Cys330) was introduced into the PPXD domain (29). Previous studies have established that an *E. coli* SecA protein lacking homologous Cys residues (SecA-C4) was active both in vivo and in vitro (33), while *B. subtilis* and *E. coli* SecA proteins deleted for 22 or 66 C-terminal residues, respectively, encompassing these Cys residues were also biologically active (33, 34).

In the SecA crystal structure Trp724 is contained within the middle of a three-helix bundle that constitutes the  $\alpha$ -helical scaffold domain that is an important domain-organizing center for SecA dimer (Figure 1). Cys282 is located at the end of an  $\alpha$ -helix, which is a major structural element within PPXD, while Cys330 is in a more weakly ordered region of PPXD. Both residues are in the portion of the PPXD domain that is proximal to the  $\alpha$ -helical scaffold domain and were accessible to sulfhydryl labeling in biologically active *E. coli* SecA mutant homologues (30). By residing within well-structured regions of their respective domains, it was our assumption that Trp724 and Cys282 should serve as good reporters of their respective domain locations.

Div-W724-C282 and Div-W724-C330 proteins were overexpressed utilizing the T7 promoter system and purified (see Experimental Procedures), and they displayed normal ATPase activities, including specific ATPase activation by *B. subtilis* SecYE protein and a gram-positive preprotein [(29); also data not shown]. They were labeled with MIANS at an efficiency of  $0.95 \pm 0.05$  (see Experimental Procedures), while Div-W724-C4 that lacks cysteine could not be labeled as judged by both absorbance and fluorescence emission [(29); also data not shown]. The MIANS-labeled proteins retained ATPase activities that were comparable to those of their unlabeled counterparts [(29); also data not shown], indicating that labeling did not perturb their biological activity.

**FRET Analysis.** The overlap between the absorption spectra of the MIANS-label and the intrinsic fluorescence emission of Trp724 (e.g., maximum at  $\sim 324$  and 330 nm, respectively) makes FRET measurements possible up to  $\sim 50$  Å, since the Förster transfer distance for MIANS-SH and Trp724,  $R_0$ , was previously shown to be  $27.8 \pm 0.2$  Å (29). A typical experiment for Div-W724-C282 and Div-W724-C330 proteins is shown in Figure 2. A decrease in Trp fluorescence emission intensity in the presence of the MIANS label was indicative of energy transfer in these two cases. The calculated distance of 25 Å for the Trp724-Cys282 spectral pair was in good agreement with the predicted intraprotomer value of 20 Å from the SecA crystal structure. The predicted interprotomer distance for the SecA dimer in this case was 76 Å, which was too large for FRET to occur. This result confirms the spatial proximity of the PPXD and C-domains of SecA in solution. Several factors would be expected to contribute to minor discrepancies between the predicted and measured values. First, our predicted distances were based on the separation between the C $\alpha$  atoms of the donor and acceptor residues because the uncertainty in the

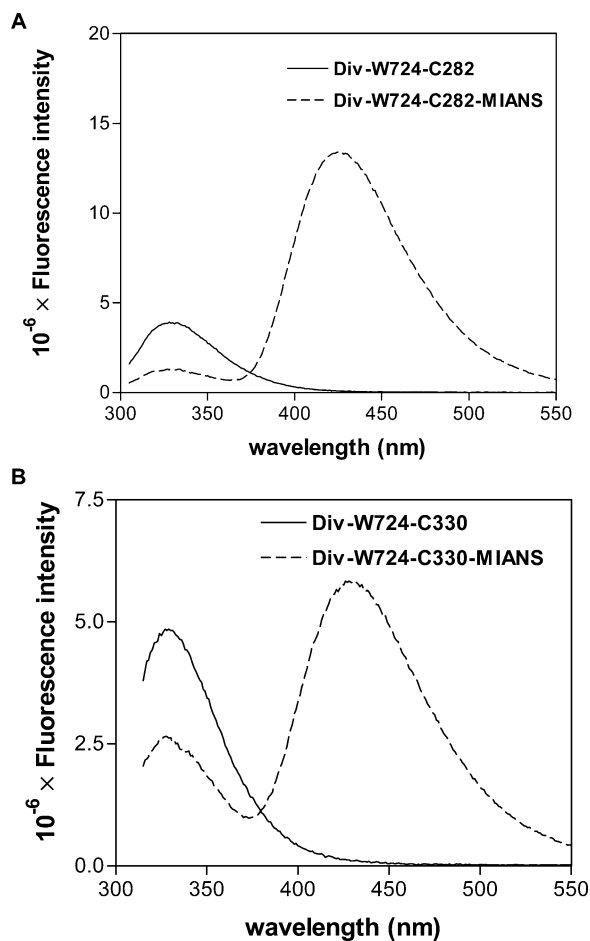
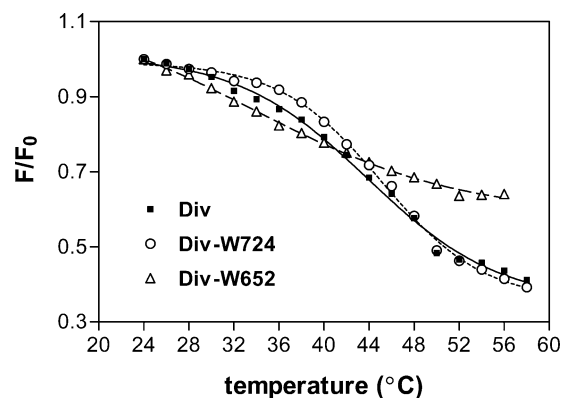


FIGURE 2: FRET analysis of mutant SecA proteins. The fluorescence emission spectra of MIANS-labeled and unlabeled SecA proteins were compared. (A) Div-W724-C282, and (B) Div-W724-C330. Fluorescent emission spectra were measured with 40  $\mu\text{g}/\text{mL}$  Div protein in TKE buffer at 24  $^{\circ}\text{C}$  using an excitation wavelength of 297 nm.

inter-fluorophore distance introduced by the dihedral flexibility of the MIANS label makes more detailed calculations unrealistic. Second, our calculations assumed a randomly oriented donor and acceptor pair (see Experimental Procedures) which may not always be the case given possible orientation biases of the probes within certain local environments.

The result with the Div-W724-C330 protein was more complex. In this case, the calculated distance of 28  $\text{\AA}$  for the Trp724-Cys330 spectral pair was significantly larger than the predicted intraprotomer value of 10  $\text{\AA}$  but much smaller than the interprotomer distance for the dimer of 59  $\text{\AA}$ . The discrepancy in this case was not unexpected, however, since Cys330 is located within a weakly ordered region of PPXD (15). Accordingly, its location within the proposed SecA crystal structure may be in error, or it may show significant mobility in solution. Furthermore, it is certainly conceivable that the MIANS label could perturb the local environment of this region or assume an orientation bias in this particular case. Given the high B factor of the PPXD domain of SecA (15) along with the requirement for selecting surface accessible residues to modify with MIANS that do not perturb SecA function, it was difficult for us to locate ideal sites within PPXD for these studies. However, this limitation was not intractable, since our studies were more



	Midpoint of transition ( $T_m$ )
Div	43.9 $\pm$ 0.5 $^{\circ}\text{C}$
Div-W724	45.1 $\pm$ 0.3 $^{\circ}\text{C}$
Div-W652	33.9 $\pm$ 1.4 $^{\circ}\text{C}$

FIGURE 3: Endothermic transition of Div, Div-W652, and Div-W724 proteins. Fluorescence emission spectra were collected every  $2 \pm 0.2$   $^{\circ}\text{C}$  with 40  $\mu\text{g}/\text{mL}$  Div protein in TKE buffer at 345 nm using an excitation wavelength of 297 nm.

focused on determining changes in FRET under different biochemical conditions rather than determining precise distances between appropriate spectral pairs.

*Dissecting the Endothermic Transition of B. subtilis SecA.* *B. subtilis* SecA normally contains two Trp residues at positions 652 and 724, corresponding to Trp701 and Trp775 of *E. coli* SecA, respectively. Trp652 is located within the  $\alpha$ -helical wing domain, while the most phylogenetically conserved Trp, Trp724, is located within the  $\alpha$ -helical scaffold domain. Using single Trp-containing mutant proteins, Div-W652 and Div-W724, we analyzed the endothermic transition of these two regions (Figure 3). Both *E. coli* and *B. subtilis* SecA proteins have been shown to undergo comparable, reversible conformational changes up to 43  $^{\circ}\text{C}$  based on their Trp fluorescence emission profile (13, 22). We have previously assigned this feature to the C-domain of SecA, which has been shown to make a conformational alteration to a state with higher mobility as indicated by fluorescence anisotropy (15, 23). Interestingly, while Div-W724 displayed a typical sigmoidal transition similar to the wild-type protein, Div-W652 showed a gradual reduction in Trp fluorescence intensity over this temperature range (akin to L-tryptophan). These results indicate that the endothermic transition of SecA as monitored by Trp fluorescence can be assigned largely to a conformational change within the Trp724 region of the  $\alpha$ -helical scaffold domain. Previous studies have shown that the homologous residue of *E. coli* SecA, Trp775, increased its solvent exposure during the endothermic transition as indicated by enhanced exposure to hydrophilic collisional quenchers (23).

*Effect of Temperature on PPXD-C-Domain Interaction.* We next addressed the effect of temperature on PPXD-C-domain association, since it seemed likely to us that this parameter may play an important role in relieving the repressive effects of the C-domain on PPXD function that have been noted previously (17, 25). Accordingly, we

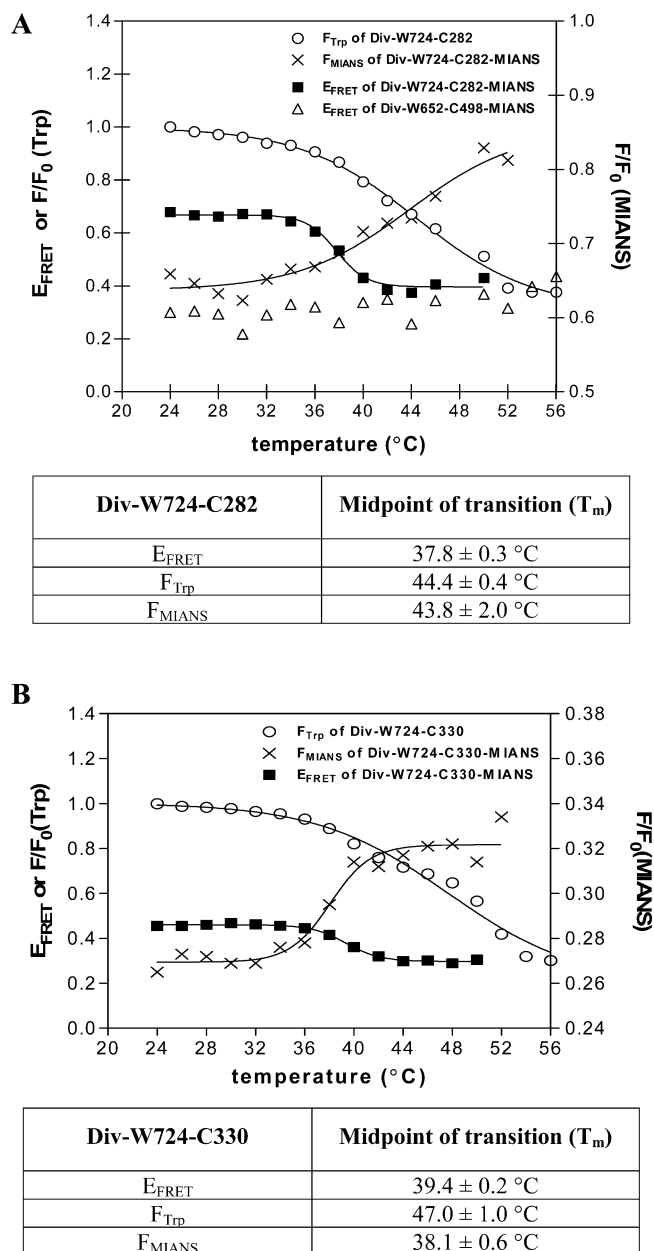


FIGURE 4: Endothermic transition of (A) Div-W724–C282 protein, and (B) Div-W724–C330 protein as monitored by FRET efficiency or Trp or MIANS fluorescence. Fluorescence emission spectra were collected every  $2 \pm 0.2$  °C with  $40 \mu\text{g/mL}$  Div protein in TKE buffer at 345 nm for Trp or 440 nm for MIANS using an excitation wavelength of 297 or 324 nm, respectively. FRET was performed similarly to Figure 2, and FRET efficiency was calculated as described in Experimental Procedures. The midpoints ( $T_m$ ) of the different endothermic transitions are given below the figure. The FRET efficiency of Div-W652–C498 protein is given in panel A for control purposes.

monitored the effect of temperature on FRET efficiency for MIANS-labeled Div-W724–C282 protein, and we also compared it to the effects of temperature on either Trp or MIANS fluorescence for this protein. Interestingly, the FRET efficiency decreased with increasing temperature, and it displayed a sigmoidal curve similar to the endothermic transition observed for Trp fluorescence but shifted to lower temperature (Figure 4A). A similar result was obtained with Div-W724–C330 protein (Figure 4B and Table 1), indicating that this pattern was not unique for the C282 region, but rather, was probably more typical of the PPXD domain as a

whole. These observations were not an artifact of our methodology as the FRET efficiency of MIANS-labeled Div-W652–C498 protein was relatively constant over this temperature range (Figure 4A). This latter protein has the MIANS label attached to the low affinity nucleotide-binding fold (NBF-II) of SecA protein, and it allows monitoring of the effect of temperature increase on NBF-II and C-domain proximity between adjacent protomers of the SecA dimer. These data indicate that there is a specific loosening in the association of the PPXD and C-domains of SecA, which may help to destabilize the C-domain at higher temperature. In addition, the curves for MIANS fluorescence versus temperature of Div-W724–C282 and Div-W724–C330 proteins were also sigmoidal in appearance with distinct  $T_m$  values (Figure 4). While the transition for the Cys282 region occurred at a temperature that was similar to that obtained for Trp fluorescence, the Cys330 region was considerably less stable and occurred at lower temperature. These latter observations were also investigated by analysis of the emission maxima (and 410/450 nm ratio) of MIANS fluorescence versus temperature for these two proteins. The data indicated that the Cys282 region was precipitously blue shifted at high temperature, while the emission maximum of the Cys330 region was more modestly and gradually blue shifted over the temperature range investigated (data not shown). These data indicate that the Cys282 and Cys330 regions differ in their temperature-induced response to the conformational change that occurs for the PPXD domain. We were unable to exclude any effect of the MIANS label on these observations, however.

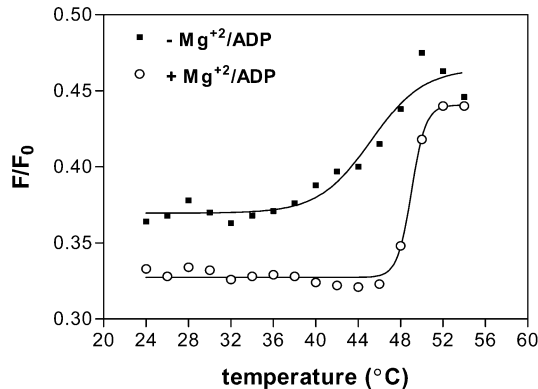
*Effect of Phospholipid Binding on PPXD–C-Domain Interaction.* The endothermic transition of SecA mimics the conformational change that is induced when SecA binds to model membranes containing anionic phospholipids (5, 13, 14). Therefore, we compared the FRET efficiency of Div-W724–C282 and Div-W724–C330 proteins in the absence and presence of LUV containing anionic phospholipids. Both proteins showed binding affinities for LUV that were similar to wild-type Div protein ( $K_d$  of  $\sim 130 \mu\text{g/mL}$ ; data not shown). In the presence of  $300 \mu\text{g/mL}$  LUV the FRET efficiency decreased for both proteins to a value that was similar to that observed at high temperature (Table 1). Furthermore, the combined effects of temperature and phospholipid binding were not additive on the FRET efficiency obtained (data not shown). These data indicate that the PPXD and C-domains respond similarly to increased temperature or binding to model membrane containing anionic phospholipids, and this response involves a loosening of the association between these two domains.

*Effect of ADP Binding on PPXD–C-Domain Interaction.* Since ADP binding to SecA has a number of effects on its overall conformation and function, including stabilizing it to proteolysis, inhibiting preprotein cross-linking, stabilizing the ground state during the endothermic transition, and affecting its overall shape as measured by dynamic light scattering (5, 22, 35), we investigated the effect that it had on PPXD and C-domain interaction. Div-W724–C282 protein displayed normal ADP-dependent stabilization of its endothermic transition ( $T_m$  of  $44.2 \pm 0.4$  °C versus  $46.5 \pm 0.6$  °C for samples without or with  $200 \mu\text{M}$  ADP, respectively, data not shown). Both Div-W724–C282 and Div-W724–C330 proteins showed increased FRET efficiencies

Table 1: FRET Results for PPXD–C-Domain Association of SecA

	$R_0$ (Å) <sup>a</sup> (± 0.2 Å)	Div-W724–C282-MIANS		Div-W724–C330-MIANS		SecA-S300C-MIANS
		$E_{\text{FRET}}^b$	$R$ (Å) <sup>c</sup>	$E_{\text{FRET}}^b$	$R$ (Å) <sup>c</sup>	$E_{\text{FRET}}^b$
alone	27.8	0.65 ± 0.01	25.1 ± 0.3	0.519 ± 0.006	27.5 ± 0.2	0.607 ± 0.008
+ LUV	28.7	0.46 ± 0.03	29.5 ± 0.8	0.462 ± 0.009	29.4 ± 0.3	0.43 ± 0.04
at high T	26.5	0.43 ± 0.03	27.8 ± 0.8	0.35 ± 0.01	29.4 ± 0.3	0.51 ± 0.03
+ Mg <sup>2+</sup> /ADP	27.2	0.71 ± 0.02	23.4 ± 0.5	0.571 ± 0.006	25.9 ± 0.1	0.63 ± 0.02

<sup>a</sup>  $R_0$  for the Trp724–MIANS pair was determined under various conditions as described in Experimental Procedures. <sup>b</sup> FRET efficiency ( $E_{\text{FRET}}$ ) was measured by decreased donor (Trp) fluorescence intensity. <sup>c</sup> Donor–acceptor distance ( $R$ ) was calculated as described in Experimental Procedures. Mean values and standard deviations are calculated from at least three FRET experiments.



Div-W724-C282-MIANS	Midpoint of transition ( $T_m$ )
- Mg <sup>2+</sup> /ADP	45.2 ± 1.0 °C
+ Mg <sup>2+</sup> /ADP	49.0 ± 0.1 °C

FIGURE 5: Effect of ADP on the endothermic transition of MIANS-labeled Div-W724–C282 protein. The experiment was performed similarly to that described in the Figure 3 legend except for the inclusion of 5 mM MgCl<sub>2</sub> and 200 μM ADP, where indicated. The midpoints ( $T_m$ ) of the different endothermic transitions are given below the figure.

in the presence of ADP (Table 1), indicating a tightening of the association of the PPXD and C-domains in this case. In addition, we noted that by monitoring MIANS fluorescence versus temperature that there was a dramatic ADP-dependent stabilization of the Cys282 region at higher temperature as inferred from the higher  $T_m$  (Figure 5). In addition, by monitoring the FRET efficiency of MIANS-labeled Div-W724–C282 versus temperature, we noted that there was a significant increase in the  $T_m$  of this parameter in the presence of ADP as well (data not shown). In sum, these and previous results suggest that ADP binding to SecA stabilizes the ground state conformation of both the PPXD and C-domains as well as tightening their association. In turn, these effects would be expected to inhibit preprotein and phospholipid binding as previously noted (14, 35).

**Parallel Studies with *E. coli* SecA Protein.** Since most of the genetic and biochemical analysis of SecA has been done with the *E. coli* system, we performed parallel studies with *E. coli* SecA protein, which is 50% identical in protein sequence to its *B. subtilis* counterpart. *E. coli* SecA protein does have the complication that it contains seven Trp residues, although only the three Trp residues located within the C-domain (Trp701, Trp723, and Trp775) contribute significantly to fluorescence (23). We have previously described an *E. coli* SecA protein, SecA-S300C, that contains a Cys residue at the homologous site to Cys282 of *B. subtilis* SecA, and which is functional in vivo (30). Purified SecA-

S300C protein displayed normal ATPase activities both before and after MIANS labeling (data not shown). Measurement of FRET efficiency between Cys300 and the Trp ensemble within the C-domain gave a basal value and pattern that was similar to that found for the two *B. subtilis* SecA proteins characterized above (Table 1). In particular, FRET efficiency was decreased at high temperature or in the presence of LUV, while it was modestly increased in the presence of ADP. We did not calculate distances in this case, however, given the complication of having multiple Trp residues within the C-domain. These results support the generality of our findings on PPXD and C-domain proximity for SecA protein and its modulation by temperature and translocation ligands.

**Relaxed PPXD and C-Domain Association in a Hyperactive Azi-PrID SecA Protein.** We have shown previously that SecA mutant proteins that are resistant to the ATPase inhibitor sodium azide (Azi) or that suppress signal sequence defects (PrID) are altered in a number of their properties. These include (i) a more open conformational state, (ii) increased membrane association, (iii) higher membrane ATPase activity, (iv) reduced affinity for ADP at NBF-I, and (v) an accelerated nucleotide-exchange rate (36). Such mutant SecA proteins can be considered hyperactive, given their ability to promote protein translocation in the presence of azide or with proteins lacking a normally functional signal peptide. To study PPXD and C-domain interaction in an Azi-PrID SecA protein, we constructed SecA-Y134S–S300C (see Experimental Procedures). The Tyr134 to Ser alteration was isolated previously as *prID21* and *prID23*, and such mutants displayed both azide resistant and signal sequence suppressor phenotypes (37). This protein is similar to SecA-Y134C (*prID22*), which displayed all of the alterations that were noted above (36), but which could not be employed here due to the Cys substitution at position 134. Comparison of SecA-S300C and SecA-Y134S–S300C proteins in an endothermic transition experiment showed that this latter protein had a lower  $T_m$  (37.4 ± 0.7 versus 42.1 ± 0.4; Figure 6), indicative of destabilization of the C-domain by the Ser134 substitution in NBF-I. A comparable result was obtained previously for the Cys134 substitution (36). Comparison of the FRET efficiency of SecA-S300C and SecA-Y134S–S300C at 24 °C showed that the Azi-PrID SecA protein had a greatly reduced value (0.61 ± 0.01 versus 0.32 ± 0.03, respectively), indicative of substantial loosening of the association of the PPXD and C-domains. The reduction obtained in this latter case was greater than that obtained for SecA-S300C at higher temperature or by addition of LUV. We assume that the genetically altered NBF-I domain destabilizes the interaction between the PPXD and C-domains

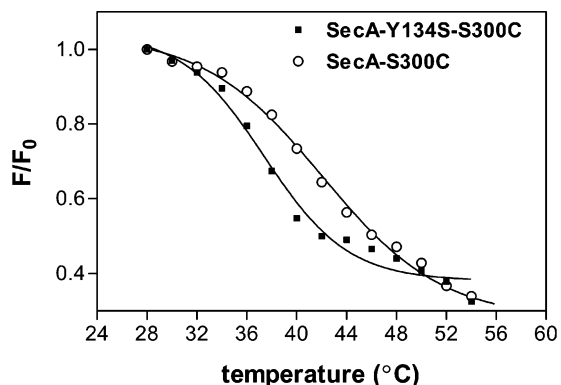


FIGURE 6: Endothermic transition of SecA-S300C and SecA-Y134S-S300C proteins. Fluorescence emission spectra were collected every  $2 \pm 0.2$  °C with 40  $\mu\text{g}/\text{mL}$  SecA protein in TKE buffer at 345 nm using an excitation wavelength of 297 nm.

by being in direct contact with both domains (15). This final result lends additional support to our hypothesis that PPXD and C-domain association and its modulation by translocation ligands plays an important role in the structural alterations needed for SecA activation.

## DISCUSSION

Previous biochemical studies indicate that soluble and membrane-bound SecA exist in different conformational states that are important for regulating the basic protein translocation cycle. While initial binding of SecA to its receptor, SecYE protein, does not appear to require a major change in SecA conformation, preprotein and SecB binding to SecA occur with significantly higher affinity in its membrane-bound state or when the repressive effects of the C-domain are removed (17, 25, 38, 39). When translocon-associated SecA is bound by both preprotein and ATP, an additional conformational change occurs that leads to the insertion of a portion of SecA into the membrane, as detected by a protease-resistance of the C-domain and the periplasmic exposure of portions of the PPXD and C-terminal linker domains to a membrane-impermeable sulfhydryl-labeling reagent (20, 30). An overall translocation cycle for SecA has been proposed where mobile regions of SecA undergo membrane insertion and retraction cycles that are coupled to the stepwise translocation of the protein substrate (20, 40). This basic model of SecA ATPase motor function has also received additional support by recognition of the amino acid and structural homology of SecA to DNA and RNA helicases of superfamily II (15, 17). However, this model has been challenged by data suggesting that protein translocation can occur from SecA that remained permanently embedded in the membrane and did not appear to undergo membrane cycling (41).

While numerous biochemical studies have charted the effects of translocation ligands on SecA function, the details of their effects on SecA structure have remained largely unknown due to the lack of a high-resolution SecA structure. This has prevented the building of a cohesive model of SecA mechanism that relates its structure and function.

In the present study, we were able to make use of our recent knowledge of SecA structure to begin to fill this gap (15, 29). We choose to initiate such studies with the PPXD and C-domains of SecA, given the profound changes that

these domains must make during the protein translocation cycle as well as studies indicating that the C-domain has repressive effects on SecA-preprotein interaction (17, 25). We also had previous evidence that the C-domain of SecA was usually structurally dynamic, based on temperature, nucleotide, phospholipid, and SecYE-dependent changes in its conformation (21–23, 42).

On the basis of examination of the *B. subtilis* SecA crystal structure, which we took as the ground state of SecA, we hypothesized that the proximity of the PPXD and C-domains might represent a mutually inhibitory interaction that was responsible for some of the biochemical observations noted above. In addition, it seemed probable to us that this tight association was likely to be relaxed through the control of various translocation ligands to achieve SecA activation for the early portions of the translocation cycle. Our data support this basic tenet in which we found that PPXD and C-domain association in soluble SecA at lower temperatures was similar to that found in the *B. subtilis* SecA crystal structure (at least for the Cys282 and Trp724 regions investigated). Modulators of the extended state of SecA (temperature, and phospholipid binding) promoted loosening of PPXD and C-domain association, while a modulator of the compact state of SecA (ADP) promoted a tightening of this association. While our study indicates that modulation of PPXD and C-domain association may play a key role in SecA activation, this basic hypothesis will need further examination in a more complete rather than a model biological system.

Additional support for our hypothesis was obtained through the characterization of a homologous *E. coli* SecA protein as well as a hyperactive Azi-PrfD SecA protein, in which PPXD and C-domain association was significantly perturbed and was presumably responsible, at least in part, for the activated state of this protein (36). This mutant has the additional complexity that the alteration in NBF-I is likely to affect interactions of this domain with the PPXD and C-domains, further complicating the basic picture.

Our study also documented conformational changes within the PPXD and C-domains of SecA protein. These conformational changes presumably enhance such processes as preprotein binding, additional SecYE interactions, and membrane insertion of at least portions of these domains under the appropriate conditions (i.e., after SecYE, preprotein, and ATP binding). Both Cys300 and Cys350 of *E. coli* SecA (corresponding to Cys282 and Cys330 of *B. subtilis* SecA) have been shown to be periplasmically accessible in membrane-inserted SecA, indicative of the complex conformational changes that need to occur within PPXD to catalyze the SecA and preprotein insertion reaction (30). It remains a challenge, however, to link each of these distinct conformational changes with the appropriate biochemical interaction and function that they induce.

On the basis of the shift in fluorescence emission maxima of MIANS with temperature, it appears that the Cys282 and Cys330 regions become more hydrophobic after their endothermic transitions. These events may induce additional exposure of a hydrophobic preprotein-binding determinant on SecA or they may promote SecA membrane interaction or insertion. In contrast, the Trp724 region becomes more solvent accessible as demonstrated previously (23), and this feature might be responsible for binding of SecA to cytoplasmic loops of SecYE protein (43), or weakening of

the interaction of this region with NBF-I that has been shown to normally repress SecA ATPase activity in the ground state (26). A cavity map of potential ligand-binding sites for SecA revealed a network of cavities at the PPXD and C-domain interface, which was suggested as a potential preprotein binding site (15). Both the PPXD and portions of the C-domain are weakly ordered so they remain suitably flexible to accommodate such ligands (15).

FRET experiments parallel to those presented here can be conducted to investigate other interdomain interactions in the SecA protomer. Examples of interesting studies could include dissection of the distinct interactions that NBF-I makes with the PPXD and C-domains, particularly given the availability and importance of the *azi* and *prlD* mutants for understanding SecA function (37). On the basis of the *Mycobacterium tuberculosis* SecA crystal structure, a model for the chemomechanical cycle of SecA protein has been presented recently that placed particular importance on two  $\beta$ -sheets connecting NBF-I with PPXD and the remarkably long  $\alpha$ -helix connecting NBF-II with the C-domain for promoting processive movement (44). Our present study highlights the value of the FRET approach for testing such a model. In addition, the study of NBF-I and NBF-II interaction should be undertaken as well, since it controls the accessibility of the high affinity nucleotide-binding site of SecA and has been proposed to regulate multiple ATP turnover events in concert with C-domain modulation (15, 45). Finally, with the recent finding of a dynamic SecA monomer-dimer equilibrium during protein translocation conditions (46-48), FRET studies could also be used to address when and how SecA monomerizes or whether an alternative dimer forms during this process. This basic approach should lend additional insight at the structural level to SecA function and mechanism.

## ACKNOWLEDGMENT

We thank Chris Zito for preparation of inverted membrane vesicles needed for the ATPase assays.

## REFERENCES

- Randall, L. L., and Hardy, S. J. S. (2002) *Cell. Mol. Life Sci.* 59, 1617-1623.
- Danese, P. N., and Silhavy, T. J. (1998) *Annu. Rev. Genet.* 32, 59-94.
- Fekkes, P., and Driessen, A. J. M. (1999) *Microbiol. Rev.* 63, 161-173.
- Mori, H., and Ito, K. (2001) *Trends Microbiol.* 9, 494-500.
- Shinkai, A., Mei, L. H., Tokuda, H., and Mizushima, S. (1991) *J. Biol. Chem.* 266, 5827-5833.
- Mitchell, C., and Oliver, D. B. (1993) *Mol. Microbiol.* 10, 483-497.
- Kimura, E., Akita, M., Matsuyama, S.-I., and Mizushima, S. (1991) *J. Biol. Chem.* 266, 6600-6606.
- Wang, L., Miller, A., and Kendall, D. A. (2000) *J. Biol. Chem.* 275, 10154-10159.
- Fekkes, P., de Wit, J. G., van der Wolk, J. P. W., Kimsey, H. H., Kumamoto, C. A., and Driessen, A. J. M. (1998) *Mol. Microbiol.* 29, 1179-1190.
- Manting, E. H., van der Does, C., and Driessen, A. J. M. (1997) *J. Bacteriol.* 179, 5699-5704.
- Nishiyama, K.-I., Suzuki, T., and Tokuda, H. (1996) *Cell* 85, 71-81.
- Mori, H., Sugiyama, H., Yamanaka, M., Sato, K., Tagaya, M., and Mizushima, S. (1998) *J. Biochem.* 124, 122-129.
- Ulbrandt, N. D., London, E., and Oliver, D. B. (1992) *J. Biol. Chem.* 267, 15184-15192.
- Breukink, E., Demel, R. A., de Korte-Kool, G., and de Kruijff, B. (1992) *Biochemistry* 31, 1119-1124.
- Hunt, J. F., Weinkauff, S., Henry, L., Fak, J. J., McNicholas, P., Oliver, D. B., and Deisenhofer, J. (2002) *Science* 297, 2018-2026.
- Matsuyama, S., Kimura, E., and Mizushima, S. (1990) *J. Biol. Chem.* 265, 8760-8765.
- Baud, C., Karamanou, S., Sianidis, G., Vrontou, E., Politou, A. S., and Economou, A. (2002) *J. Biol. Chem.* 277, 13724-13731.
- Breukink, E., Nouwen, N., van Raalte, A., Mizushima, S., Tommassen, J., and de Kruijff, B. (1995) *J. Biol. Chem.* 270, 7902-7907.
- Kourtz, L., and Oliver, D. (2000) *Mol. Microbiol.* 37, 1342-1356.
- Economou, A., and Wickner, W. (1994) *Cell* 78, 835-843.
- Eichler, J., Brunner, J., and Wickner, W. (1997) *EMBO J.* 16, 2188-2196.
- den Blaauwen, T., Fekkes, P., de Wit, J. G., Kuiper, W., and Driessen, A. J. M. (1996) *Biochemistry* 35, 11994-12004.
- Ding, H., Mukerji, I., and Oliver, D. (2001) *Biochemistry* 40, 1835-1843.
- Song, M., and Hyounghan, K. (1997) *J. Biochem.* 122, 1010-1018.
- Triplett, T. L., Sgrignoli, A. R., Gao, F.-B., Yang, Y.-B., Tai, P. C., and Gierasch, L. M. (2001) *J. Biol. Chem.* 276, 19648-19655.
- Karamanou, S., Vrontou, E., Sianidis, G., Baud, C., Roos, T., Kuhn, A., Politou, A. S., and Economou, A. (1999) *Mol. Microbiol.* 35, 1133-1145.
- Dong, W. J., Xing, J., Robinson, J. M., and Cheung, H. C. (2001) *J. Mol. Biol.* 314, 51-61.
- Trakselis, M. A., Alley, S. C., Abel-Santos, E., and Benkovic, S. J. (2001) *Proc. Natl. Acad. Sci. U.S.A.* 98, 8368-8375.
- Ding, H., Hunt, J. F., Mukerji, I., and Oliver, D. (2003) *Biochemistry* 42, 8729-8738.
- Ramamurthy, V., and Oliver, D. (1997) *J. Biol. Chem.* 272, 23239-23246.
- Lanzetta, P. A., Alvarez, L. J., Reinach, P. S., and Candia, O. A. (1979) *Anal. Biochem.* 100, 95-97.
- Lakowicz, J. R. (1999) in *Principles of Fluorescence Spectroscopy*, 2nd ed., pp 367-394, Plenum Publishers, New York.
- Rajapandi, T., and Oliver, D. (1994) *Biochem. Biophys. Res. Commun.* 200, 1477-2483.
- van Wely, K., Swaving, J., Klein, M., Freudl, R., and Driessen, A. (2000) *Microbiology* 146, 2573-2581.
- van Voorst, F., Vereyken, I. J., and de Kruijff, B. (2000) *FEBS Lett.* 486, 57-62.
- Schmidt, M., Ding, H., Ramamurthy, V., Mukerji, I., and Oliver, D. (2000) *J. Biol. Chem.* 275, 15440-15448.
- Huie, J., and Silhavy, T. (1995) *J. Bacteriol.* 177, 3518-3526.
- Hartl, F.-U., Lecker, S., Schiebel, E., Hendrick, J. P., and Wickner, W. (1990) *Cell* 63, 269-279.
- den Blaauwen, T., Terpetschnig, E., Lakowicz, J., and Driessen, A. (1997) *FEBS Lett.* 416, 35-38.
- van der Wolk, J. P. W., de Wit, J. G., and Driessen, A. J. M. (1997) *EMBO J.* 16, 7297-7304.
- Chen, X., Xu, H., and Tai, P. (1996) *J. Biol. Chem.* 271, 29698-29706.
- van der Does, C., Manting, E. H., Kaufmann, A., Lutz, M., and Driessen, A. J. M. (1998) *Biochemistry* 37, 201-210.
- Matsumoto, G., Yoshihisa, T., and Ito, K. (1997) *EMBO J.* 16, 6384-6393.
- Sharma, V., Arockiasamy, A., Ronning, D. R., Savva, C. G., Holzenburg, A., Braunstein, M., Jacobs, W. R., and Sacchettini, J. C. (2003) *Proc. Natl. Acad. Sci. U.S.A.* 100, 2243-2248.
- Sianidis, G., Karamanou, S., Vrontou, E., Boulias, K., Repanas, K., Kyripides, N., Politou, A. S., and Economou, A. (2001) *EMBO J.* 20, 961-970.
- Woodbury, R. L., Hardy, S., and Randall, L. (2002) *Protein Sci.* 11, 875-882.
- Or, E., Navon, A., and Rapoport, T. (2002) *EMBO J.* 21, 4470-4479.
- Benach, J., Chou, Y.-T., Fak, J. J., Itkin, A., Nicolae, D. D., Smith, P. C., Wittrock, G., Floyd, D. L., Golsaz, C. M., Gierasch, L. M., and Hunt, J. F. (2002) *J. Biol. Chem.* 278, 3628-3638.